RSC Advances

ROYAL SOCIETY OF CHEMISTRY

www.rsc.org/advances

Effect of *pre*-imidization on the structures and properties of polyimide fibers

Jingjing Chang,[a] Qiyan Ge,[a] Mengying Zhang,[a] Weiwei Liu,[a] Li Cao,[a] Hongqing Niu,*[b] Gang Sui[b] and Dezhen Wu*[a]

Graphical and Textual Abstract

The *pre*-imidization process was adopted in preparing high-performance polyimide fibers, resulting in the effectively improved mechanical properties of the resultant polyimide fibers.

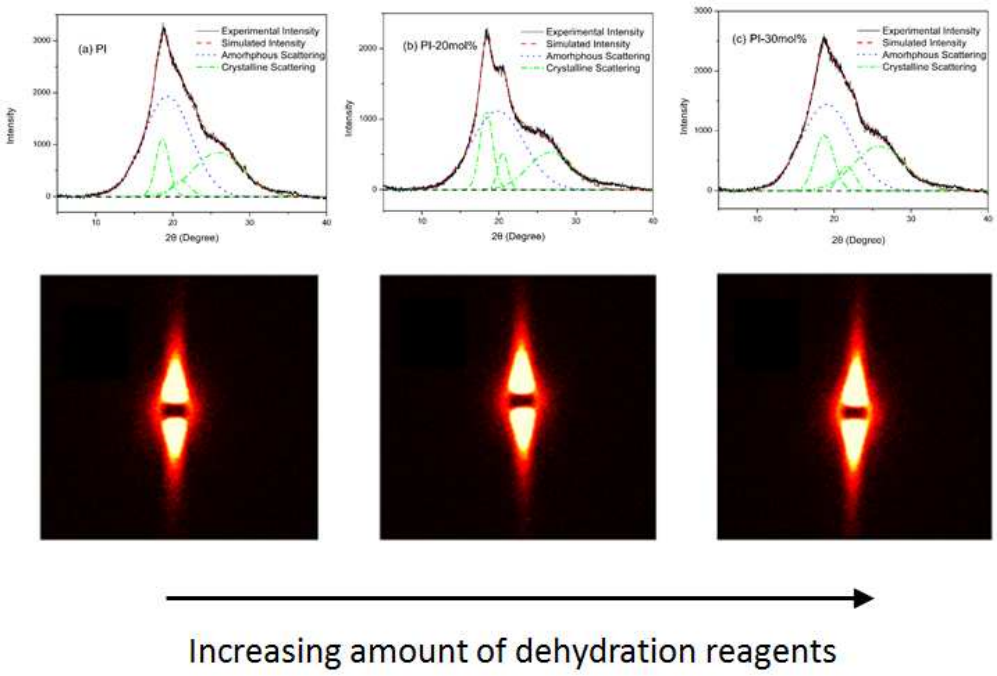

Effect of *pre*-imidization on the structures and properties of polyimide fibers

Jingjing Chang,[a] Qiyan Ge,[a] Mengying Zhang,[a] Weiwei Liu,[a] Li Cao,[a] Hongqing Niu,*[b] Gang Sui[b] and Dezhen Wu*[a]

[a] State Key Laboratory of Chemical Resource Engineering, College of Materials Science and Engineering, Beijing University of Chemical Technology, Beijing 100029, China

Corresponding author. Tel. /fax: +86 10 6442 1693.

E-mail address: wdz@mail.buct.edu.cn (Dezhen Wu).

[b] Key Laboratory of Carbon Fiber and Functional Polymers, Ministry of Education, Beijing University of Chemical Technology, Beijing 100029, China

Corresponding author. Tel. /fax: +86 10 6442 4654.

E-mail address: niuhq@mail.buct.edu.cn (Hongqing Niu).

ABSTRACT

A series of polyimide (PI) fibers derived from 3,3',4,4'-biphenyltetracarboxylic dianhydride (BPDA), 4,4'-oxydiphthalic anhydride (ODPA) and *p*-phenylenediamine (*p*-PDA) were successfully prepared through a partially *pre*-imidization process, and the effects of different amount of dehydration reagents and initial poly (amic acid) (PAA) concentrations on the structure-property relationship of the resultant PI fibers were systematically investigated. The results showed that both the increased amount of dehydration reagents and PAA concentration could result in the ordered molecular packing arrangement of the polymer chains and gradually formed homogeneous structures in the fibers, which are proposed to be essentially dominated for the

effectively enhancement in the mechanical properties of PI fibers. Moreover, the PI fibers obtained through the *pre*-imidization process still exhibited excellent thermal-oxidative stabilities, although the 5 % weight loss temperature of the PI fibers was slightly decreased compared with that of the pure PI fibers as a result of the residual dehydration reagents in the fibers. Consequently, the present work provided a new approach in preparing high-performance PI fibers through a partially *pre*-imidization process.

Keywords: *pre*-imidization; polyimide fibers; molecular packing; morphology

1 Introduction

As one of the most promising materials in the class of high-performance polymeric fibers, aromatic polyimide (PI) fibers have drawn much attentions due to the excellent mechanical properties, outstanding thermal-oxidative stabilities, superior chemical and irradiation resistance as well as good dielectric performances.[1-4] In this regard, they have been extensively applied into widespread areas such as microelectronics, engineering and aerospace industry.[5-8] Although the development of high-performance PI fibers have made significant progresses in the past decades, the properties of the resultant PI fibers are still in need of further improvement when employed in severer circumstances or being the substitution for the other products.[9, 10] Therefore, lots of research works were carried out with the aim of obtaining PI fibers with outstanding performances.

Recently, a typical two-step method is mainly adopted in preparing PI fibers, in which poly (amic acid) (PAA) fibers are obtained by extruding PAA solution into coagulation bath and subsequently converted into corresponding PI fibers through thermal or chemical imidization process.[11, 12] Taking advantage of the extensive amount of monomers to be copolymerized, much efforts have been paid to incorporate the monomers with specific groups into the polymer backbone in order to combine the advantages of individual group.[13-15] For example, Niu et al. have introduced the monomer 2-(4-aminophenyl)-6-amino-4(3H)-quinazolinone (AAQ) into the 3,3',4,4'-biphenyltetracarboxylic dianhydride (BPDA) /*p*-phenylenediamine (*p*-PDA) backbone to obtain the PI fibers with the tensile strength and initial modulus up to 2.8 and 115.2 GPa, respectively.[10] The incorporation of rigid-rod heterocyclic units containing both –NH– and =N– has enhanced the intermolecular associations, which was proposed to affect the mechanical properties of PI fibers. However, as for two-step wet-spinning method, some defects such as microvoids could be generated during dual-diffusion and thermal imidization process.[16-19] It was reported that the incorporated 4,4'-oxydiphthalic anhydride (ODPA) moieties into the BPDA/*p*-PDA polymer backbone resulted in the reduced size of the microvoids in the fibers, which was the main reason for the dramatically enhancement in the mechanical properties of the fibers.[20] Therefore, controlling the size of microvoids is especially essential in determining the final performance of the PI fibers. Moreover, it is found that the problem could be solved if the PAA solutions are *pre*-imidized before spinning into as-spun PAA fibers and consequently, the presence of the removal of micromolecules will be reduced during thermal imidization process. On the other hand, on the basis of the works related to *pre*-imidization of PI films, it can be speculated that the *pre*-imidized rigid PI units will

proceed molecular ordering with external drawing to form regular molecular arrangement, resulting in the enhancement in the properties of PI fibers.[21-23] In summary, the previous works were mainly focused on changing the chemical structures of PI fibers to modify the chemical structure of the PI fibers, while the reports related to the effect of *pre*-imidization of PAA solutions on the final performances of the PI fibers have been involved little.

In the present work, we proposed an approach in preparing BPDA/ODPA/*p*-PDA copolyimide fibers via a two-step wet-spinning method, that was, the partially *pre*-imidization process of PAA solutions by a chemical imidization method. The PAA solutions were partially *pre*-imidized by the introduction of dehydration reagents (the mixture of acetic anhydride and pyridine) to obtain PAA-PI precursors. After spinning into PAA-PI fibers, the fibers were converted into corresponding PI fibers through thermal imidization process. Herein, the effects of different amount of dehydration reagents and different PAA concentrations on the structures and properties of the final PI fibers are systematically investigated.

2 Experimental

2.1 Materials

The monomers BPDA and ODPA were supplied by Shi Jiazhuang Hai Li Chemical Company, and purified by sublimation prior to use. The monomer *p*-PDA was obtained from Shangyu Li Xing Chemical Company and purified by recrystallization. The reagents dimethylacetamide (DMAc), acetic anhydride and pyridine (analytical pure)

were purchased from Tianjin Fu Chen Chemicals Reagent Factory and used without further treatment. The deionized water used in the experiment was prepared by the Laboratory Water Purification System.

2.2 Preparation of PAA-PI solutions with different amount of dehydration reagents

In a three-necked flask equipped with a mechanical stirrer, the mixture of the dianhydrides BPDA and ODPA were added in several portions to a solution of *p*-PDA in DMAc solvent at room temperature (the molar ratio of BPDA/ODPA/*p*-PDA is 7/3/10). After stirring for 5h, the viscous spinning solution containing 12 wt% solid content was obtained. The PAA solution was divided equally into three portions, and then different amount (0, 20 and 30 mol% relative to the original amino groups) of dehydration reagents were added into the PAA solutions. The reaction mixtures were stirred for 3h at room temperature to yield homogeneous PAA-PI solutions with different imidization degrees (IDs).

2.3 Preparation of PAA-PI solutions with different PAA concentrations

Using the same procedure as described above, the PAA solution derived from BPDA, ODPA and *p*-PDA (the molar ratio of BPDA/ODPA/*p*-PDA is 7/3/10) with initial concentration of 20 wt% was obtained. Then the PAA solution was diluted to different concentrations (10, 13, 16 and 19 wt%) before use. Another 1 h later with stirring, 20 mol% dehydration reagents were added into the PAA solutions. Accordingly, the

reaction mixtures were stirred for 3h at room temperature to yield partially imidized PAA-PI solutions with different PAA concentrations.

2.4 Preparation of PI fibers

The PI fibers were prepared by the two-step wet-spinning method according to the following procedures. The PAA solution, filtrated and degassed prior to use, was extruded into the coagulation bath through a spinneret (120 holes, 70 μm in diameter) to get as-spun PAA fibers under the pressure of nitrogen. After washed by deionized water to remove the residual solvents in the fibers, the PAA fibers were dried with the oven at the temperature of 80 °C, and then were delivered into ovens with the temperatures ranging from 280 to 500 °C with concomitant drawing on the spinning rollers. The mechanical properties of PI fibers were improved extensively through the thermal imidization process. The synthetic route is illustrated in Scheme 1.

The synthesized PI (PAA) fibers with different amount of dehydration reagents of 0, 20 and 30 mol% were abbreviated as PI (PAA), PI (PAA)-20 mol% and PI (PAA)-30 mol%, respectively. The PI (PAA) fibers with different concentration of 10, 13, 16 and 19 wt% were abbreviated as PI (PAA)-10 wt%, PI (PAA)-13 wt%, PI (PAA)-16 wt% and PI (PAA)-19 wt%, respectively.

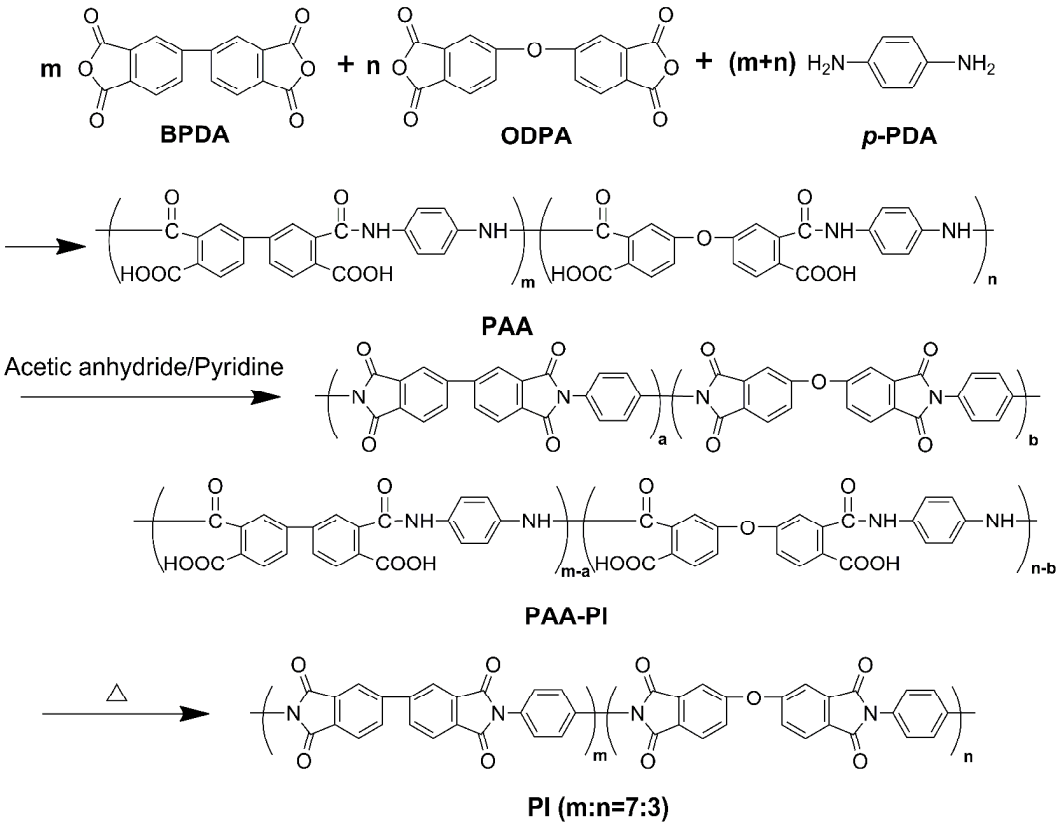

Scheme 1 The synthetic route of PI fibers

2.5 Characterization

The fourier transform infrared (FT-IR) measurements were carried out on Nexus 670 made by Nicolet Company with the scanning wavenumber ranging from 4000 to 400 cm^{-1} and average 32 scans. The samples were prepared by grinding the fibers with KBr in the mortar, and the measurements were conducted in the ambient atmosphere. Generally, the band at 1364 cm^{-1} (C-N-C stretching) is selected for quantifying the ID of the fibers, and the aromatic band at 1510 cm^{-1} (C-C stretching of the *p*-substituted benzene backbone) is selected as the internal standard. Thus, the ID can be calculated using the equation:

$$ID(\%) = \frac{(S_{1364}/S_{1510})_p}{(S_{1364}/S_{1510})_c} \times 100\% \quad (1)$$

where S is the area of the absorption band, and subscript p and c represent precursor fibers and the fully cured PI fibers, respectively.[24]

The intrinsic viscosities of the PAA solutions were measured using a Germany SCHOTT 52510 Ubbelohde viscometer at 35 °C.

The mechanical properties of PI fibers were conducted on the Instron 3344 instrument with a gauge length and extension speed of 250 mm and 125 mm min^{-1}, respectively. For each group of fibers, at least 15 filaments were tested and the average value was used as the representative.

Wide angel X-ray diffraction (WAXD) was performed using a Bruker AXS D8 ADVANCE X-ray diffractometer (Karlsruhe, Germany) in the 5-40° at a scanning rate of 10° min^{-1}. X-ray diffraction measurements were taken at room temperature using Ni-filtered Cu Kα (λ = 0.154 nm) radiation operated at 40 kV and 40 mA. The order degree X of macromolecule can be confirmed by the equation:

$$X = \frac{U_0}{I_0} \times \frac{I_X}{U_X} \times 100\% \quad (2)$$

where U_0 and U_X denote to the backgrounds of the reference sample and experimental sample, and I_0 and I_X are integral intensities of diffraction lines of the reference sample and experimental sample, respectively.[25, 26] Curve-fitting deconvolution of the WAXD profiles was performed using Origin 8.5 software to separate crystallization and amorphous contributions. The crystallinity (X_c) was calculated with the following equation:

$$X_c = \frac{A_c}{A_c + A_a} \times 100\% \quad (3)$$

where A_c and A_a represent the area of all the crystal peaks and the area of the amorphous peak, respectively.[17, 27]

Two-dimensional small angle X-ray scattering (2D SAXS) was performed on NanoSTAR-U (BRUKER AXS INC) using an HI-STAR detector. The generator was operated at 40 kV and 650 μA with Cu Kα radiation. The distance between the sample and the detector was L_{SD} = 1074 mm. The effective scattering vector q ($q=4\pi sin\theta/\lambda$, where 2θ is the scattering angle) at this distance ranging from 0.044 to 2.0 nm^{-1}.

As for wet-spinning process, the needle-shaped microvoids along the fiber axial direction were characterized by SAXS. The radius of the microvoids can be described by Guinier functions as follows:

$$I(q) = I_0 \exp(\frac{-q^2 R^2}{5}) \quad (4)$$

where R is the radius of the microvoids with circle cross-section and $I(q)$ is the scattering intensity in reciprocal. Through the Fankuchen successive tangent method, the average radius of the microvoids can be calculated on the basis of the equation:

$$R = \sum R_i W_i \left(i = 1, 2, 3\ldots\right) \quad (5)$$

where R_i is the radius of different size of the microvoids and W_i is the corresponding volume percentage of the microvoids. Then the average fibril length L and misorientation width B_Φ are determined by the following equation proposed by Ruland:

$$s^2 B_{obs}{}^2 = \frac{1}{L^2} + s^2 B_\phi{}^2 \quad (6)$$

where B_{obs} is the angular spread of the data fitting by Gaussian-Gaussian function and s is the scattering vector ($s=2sin\theta/\lambda$).

Thermo gravimetric analysis (TGA) was performed with a TGA Q50 instrument at a heating rate of 10 °C min^{-1} from 50 to 700 °C. The samples weighing about 5.0 mg were tested in nitrogen.

3 Results and Discussion

3.1 Effect of different amount of dehydration reagents on the structures and properties of polyimide fibers

3.1.1 FT-IR analysis

In general, aromatic PI fibers are synthesized from the polycondensation of dianhydrides and diamines via the two-step method. The precursor PAA fibers are then converted into final PI fibers by thermal or chemical imidization process. In the present work, both the thermal and chemical imidization process were combined to get PI fibers through the *pre*-imidization of PAA solutions. The chemical structures of the PAA and final PI fibers prepared with different amount of dehydration reagents are shown in Fig. 1(a) and 1(b), respectively. It can be seen that in Fig. 1(a), the intensity of characteristic absorption bands of PAA (1655 cm^{-1} for amide-I band and 1548 cm^{-1} for amide-II band) decreases gradually after the addition of dehydration reagents. Also, the intensity of characteristic absorption bands of PI (1773 cm^{-1} for C=O asymmetrical stretching, 1715 cm^{-1} for C=O symmetrical stretching, 1364 cm^{-1} for C-N stretching and 734 cm^{-1} for C=O bending of imide ring) increases obviously, indicating that the PAA fibers were *pre*-imidized. [28] Moreover, the characteristic absorption band of isoimide groups at

1800 cm^{-1} is not detected in the spectra, suggesting that the main product prepared in the present work is PAA-PI precursor, and the isoimide could be ignored.[21] As for PI fibers presented in Fig. 1(b), all the fibers exhibit the same absorption bands, indicating the same chemical structures of final PI fibers.

Based on the equation given in eqn (1), the IDs of the PAA and final PI fibers were calculated as summarized in Table 1. The experimental IDs of PAA fibers are close to the theoretical ones, suggesting that the IDs could be controlled by adding appropriate amount of dehydration reagents, which is favorable to obtain partially imidized PAA fibers. For PI fibers, the resulting PI fibers exhibit high imidization degrees which are all almost 100 %, promising the prepared PI fibers with excellent mechanical performances.

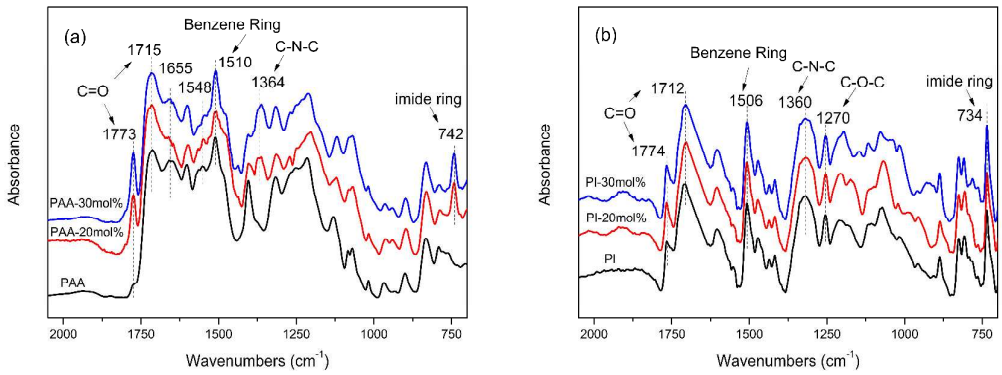

Fig. 1 FT-IR curves of the (a) PAA and (b) PI fibers with different amount of dehydration reagents

3.1.2 Mechanical properties

Table 1 depicts the IDs, intrinsic viscosities of the PAA solutions, linear density and mechanical properties of the corresponding PI fibers prepared with different amount of

dehydration reagents, in which it can be observed that the mechanical properties of PI fibers are improved with the increased amount of dehydration reagents. The pure PI fibers possess the tensile strength and initial modulus of 1.39 and 90.5 GPa, while the value increases to 1.61 and 106.24 GPa, respectively. According to the previous research, the enhancement in the mechanical properties of PI fibers is speculated to be mainly attributed to the following two factors: (a) increased ordered packing structures; (b) gradually formed homogeneous structures.[19, 21] On the other hand, it can be mentioned that in the present work, the intrinsic viscosities of the PAA-PI solutions are reduced as compared with those of pure PAA solution. It is because that the dehydration reagents are not only the imidization accelerator but also diluters when adding them into the PAA solutions. [23] Also, the apparent viscosities of the PAA solutions increase simultaneously with the addition of dehydration reagents (not shown), while excessive amount of dehydration reagents could lead to gel. Moreover, the linear density of the resulting PI fibers is found to decrease along with the reduced intrinsic viscosities of the PAA solutions. It is suggested that the molecule chains are easily drawn by external forces with regard to low intrinsic viscosities of PAA solutions. However, the intrinsic viscosity and linear density are not the main reasons for the improved mechanical performances of the PI fibers.

Table 1 The IDs, intrinsic viscosities of the PAA solutions, linear density and mechanical properties of the corresponding PI fibers with different amount of dehydration reagents

Type of PAA solution	ID of PAA fibers (%)	ID of PI fibers (%)	Intrinsic Viscosity (dL g^{-1})	Linear Density [a] (dtex)	Mechanical properties of the PI fibers		
					Tensile Strength (GPa)	Initial Modulus (GPa)	Elongation (%)
PAA	0	100	2.86	176.0	1.39±0.08	90.5±1.2	1.64±0.11
PAA+20 mol% dehydration reagents	18.5	97.8	1.91	125.0	1.57±0.13	101.9±2.7	1.60±0.15
PAA+30 mol% dehydration reagents	25.3	98.4	2.04	165.0	1.61±0.06	106.2±2.2	1.55±0.05

[a] Linear Density: The weight of a bundle of fibers with the length of 10,000 m.

3.1.3 Molecular packing

As we know, the order degree and crystallinity of macromolecules are two crucial factors that exert considerable effects on the comprehensive performances of the resultant PI fibers. The aggregation structures of the PAA fibers were characterized by WAXD as displayed in Fig. 2. All the fibers exhibit a very weak and broad peak representing a typical amorphous morphology, while the PAA-PI fibers exhibit a weak peak at 29.3 ° demonstrating a certain extent of ordered arrangement of the macromolecules after the addition of dehydration reagents. Accordingly, the order degree *X* of the macromolecules could be quantitatively calculated based on eqn (2). The corresponding order degree value of PAA, PAA-20 mol% and PAA-30 mol% fibers is 3.46 U_0/I_0, 4.90 U_0/I_0 and 5.16 U_0/I_0, respectively, giving evidence of increased displacement packing order of polymer chains with *pre*-imidization process.

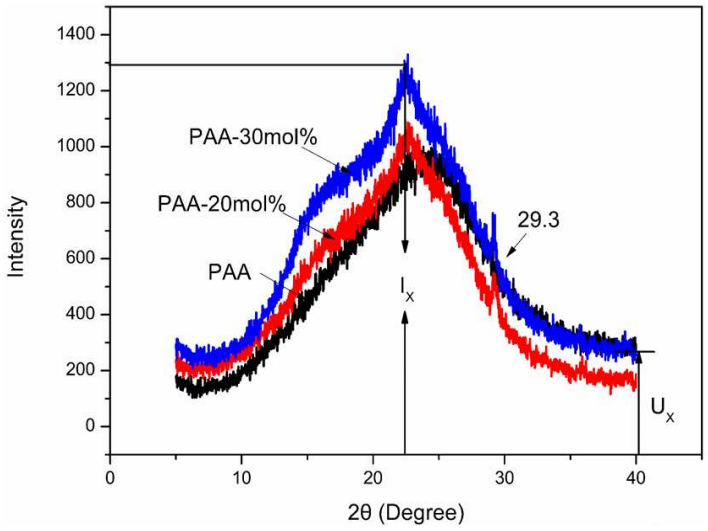

Fig. 2 The WAXD profiles of the PAA fibers with different amount of dehydration reagents

For PI fibers, substantial changes are also observed as shown in Fig. 3. All the PI fibers exhibit strong diffraction peaks in the range of 5-40°, indicating the different crystallization behavior through thermal imidization process. To further examine and intepret the crystallization behavior, the curve-fitting deconvolution of WAXD profiles was performed to separate the crystallization and amorphous contributions. Followed by the eqn (3), the crystallinity of all the samples was determined to be 35.7, 37.2 and 42.0 % for PI, PI-20 mol% and PI-30 mol% fibers, respectively. It can be explained as that with the increased amount of dehydration reagents, more rigid PI chains are generated in the PAA-PI precursors, which gradually limit the mobility of the polymer chains. Meanwhile, the *pre*-imidized PI chains will be preserved to induce the formation of more oriented structures with the contribution of thermal imidization process. Consequently, the suppressed mobility of the polymer chains and initially oriented structures together are responsible for the ordered molecular packing structures in the fibers. Hence the PI fibers prepared with the *pre*-imidization process have better molecular arrangement, which is helpful to improve the mechanical properties of PI fibers.

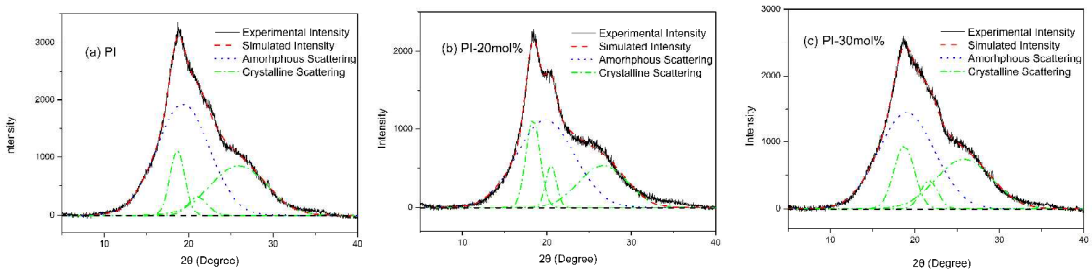

Fig. 3 The WAXD peak fitting profiles of the PI fibers with different amount of dehydration reagents

3.1.4 Morphology

The surface morphologies (a-c) of the PI fibers and fractured cross-section morphologies (d-f) of the PAA fibers with different amount of dehydration reagents are shown in Fig. 4. It can be observed that all the fibers exhibit smooth surface with different amount of dehydration reagents, indicating that the *pre*-imidization process has rarely influenced the surface morphologies of the PI fibers. From the cross-section images, all the PAA fibers possess dense morphologies without obvious microvoids structures. Meanwhile, the shape of the fibers gradually ranges from kidney to regular circle due to the quick dual-diffusion process in the coagulation bath. For *pre*-imidized PAA-PI fibers, the presence of rigid PI chains favors the removal of solvent during dual-diffusion process owing to the relatively poor affinity and therefore, the inner and outer force in the fibers tend to reach equilibrium to form regular circle morphologies. Above all, the fibers exhibit homogeneous surface as well as dense cross-section morphologies, promising the prepared PI fibers with excellent mechanical performances in the *pre*-imidization process.

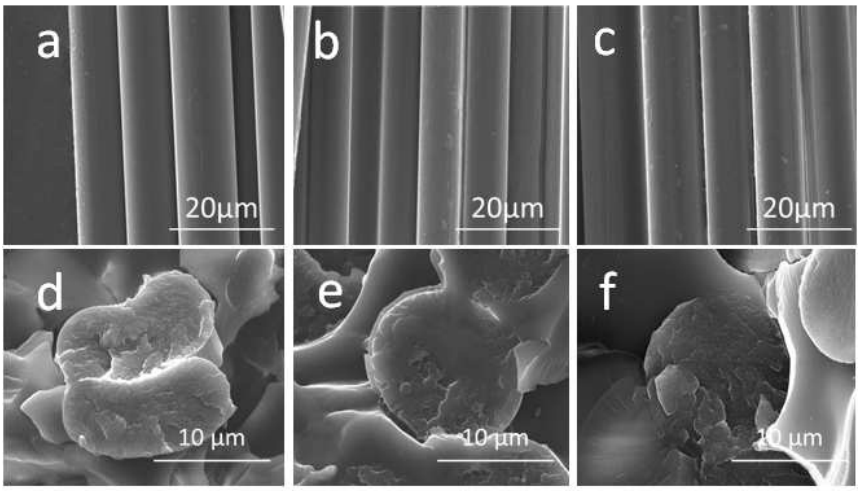

Fig. 4 The surface morphologies (a-c) of the PI fibers and fractured cross-section morphologies (d-f) of PAA fibers with different amount of dehydration reagents.

(a) PI; (b) PI-20 mol%; (c) PI-30 mol%; (d) PAA; (e) PAA-20 mol%; (f) PAA-30 mol%

Moreover, it is well known that the microvoids generated in a typical two-step wet-spinning method will greatly affect the final performances of the PI fibers. Therefore, with the purpose of obtaining high-performance PI fibers, the *pre*-imidization process was adopted to diminish the unexpected phenomenon and the structural evolution in the fibers was investigated by SAXS. Also, the parameters of microvoids such as average radius R, length L and misorientation B_{Φ} could be evaluated. From the 2D SAXS patterns of the PI fibers with different amount of dehydration reagents in Fig. 5, it can be observed that all the fibers exhibit sharp and elongated scattering streaks, demonstrating the presence of microvoids in the fibers. Meanwhile, the needle-shaped microvoids are distributed approximately parallel to the fiber axis.[20, 29]

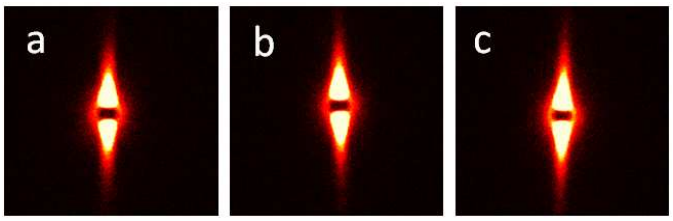

Fig. 5 2D SAXS patterns of the PI fibers with different amount of dehydration reagents.

(a) PI; (b) PI-20 mol%; (c) PI-30 mol%

The SAXS profiles of the PI fibers with different amount of dehydration reagents are shown in Fig. 6(a). The strong scattering near the beamstop indicates the

existence of nanoscale structures in the fibers. As reported by Jiang et al., the radius of the microvoids can be determined by Guinier function as shown in eqn (4). [30, 31] The radius R_i (i=1,2,3) and corresponding volume percentage W_i (i=1,2,3) to different size of microvoids can be confirmed by Fankuchen successive tangent method.[32] Accordingly, the average radius R of microvoids can be calculated according to eqn (5), and the results are listed in Table 2. The Guinier plot of the scattered intensities of PI-20 mol% fibers along the meridian direction by Fankuchen successive tangent method is also displayed in Fig. 6(b). Besides, it can be noted the scattering intensity of the microvoids decreases as a function of scattering angles, implying that the length of microvoids is not constant, that is, both the size distribution and misorientation of microvoids have contributed to the streak profiles.[33] The average fibril length L and misorientation B_Φ could be calculated by eqn (6) proposed by Ruland, while the length L is obtained from the intercept of the $\boldsymbol{s}^2 B_{obs}^2$ vs. $\boldsymbol{s}^2$ plot and misorientation B_Φ from the slope of the plot.[34, 35] The Intensity profiles corresponding to azimuthal scans at different scattering vectors and Ruland plot of the PI-20 mol% fibers are shown in Fig. 6(c) and 6(d), respectively. From the results in Table 2, there is no doubt that the addition of dehydration reagents leads to the reduced radius, length and misorientation of microvoids in the fibers, since some *pre*-imidized PI units are obtained before wet-spinning process. As a result, the gradually formed homogeneous structures promote the enhancement in the mechanical properties of PI fibers.

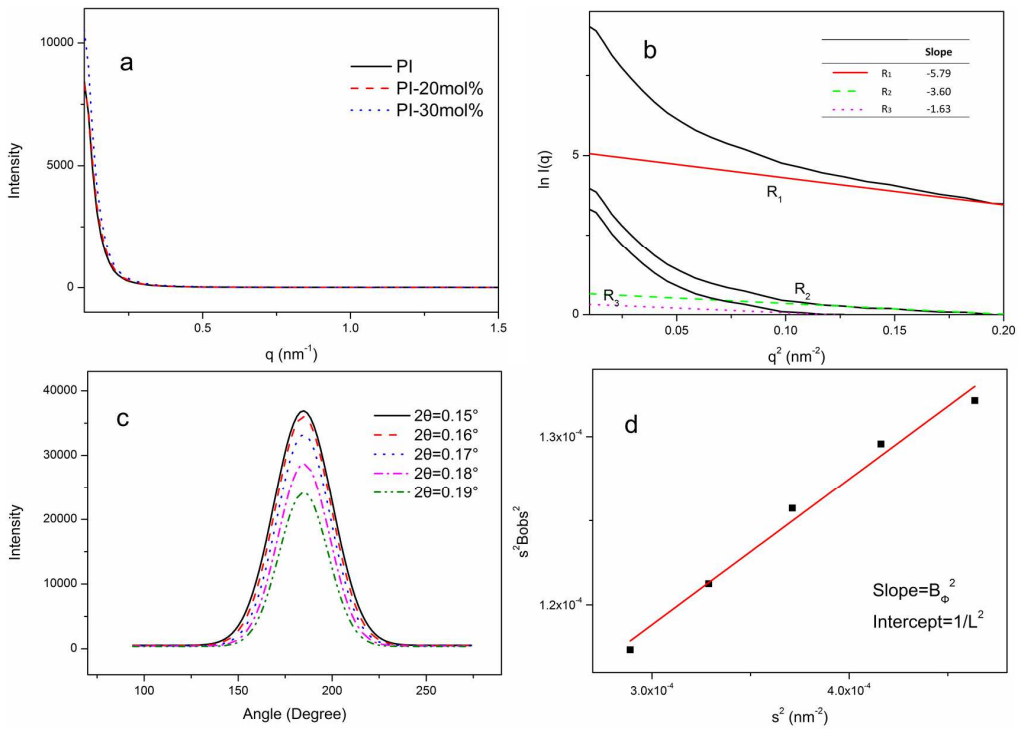

Fig. 6 (a) SAXS profiles of the PI fibers with different amount of dehydration reagents; (b) Guinier plot of the scattered intensities of PI-20 mol% fibers along the meridian direction by Fankuchen successive tangent method; (c) Intensity profiles corresponding to azimuthal scans at different scattering vectors of the PI-20 mol% fibers; (d) Ruland plot of the PI-20 mol% fibers

Table 2 The parameters of microvoids of the PI fibers with different amount of dehydration reagents

PI Fibers	R_i						R (nm)	L (nm)	B_Φ (°)
	R_1 (nm)	W_1	R_2 (nm)	W_2	R_3 (nm)	W_3			
PI	1.84	1.00	1.80	0.19	1.33	0.15	2.38	104.52	17.79
PI-20 mol%	1.63	1.00	2.06	0.12	1.09	0.15	2.03	103.75	17.03
PI-30 mol%	0.95	1.00	2.37	0.02	0.90	0.07	1.06	103.42	16.85

3.1.5 Thermal properties

The thermal-oxidative stabilities of the PI fibers with different amount of dehydration reagents were evaluated by TGA measurements in nitrogen atmosphere as illustrated in Fig. 7. All the fibers show rapid decomposition when the temperature is over 550 °C, and the char yield at 700 °C is over 60 %, indicating that the PI fibers prepared in two-step wet-spinning method exhibit excellent thermal stabilities. In addition, the T_{d5} (5 % weight loss temperature) of the PI fibers obtained from the *pre*-imidized PAA-PI solutions shows a slight decrease as compared with that of pure PI fibers. The slight reduction is induced by the residual dehydration reagents in the fibers, which promotes the decomposition of PI chains. Besides, the slight increase in T_{d5} between PI-20 mol% and PI-30 mol% fibers is strongly dependent on the increased imidization degree of the PI fibers.

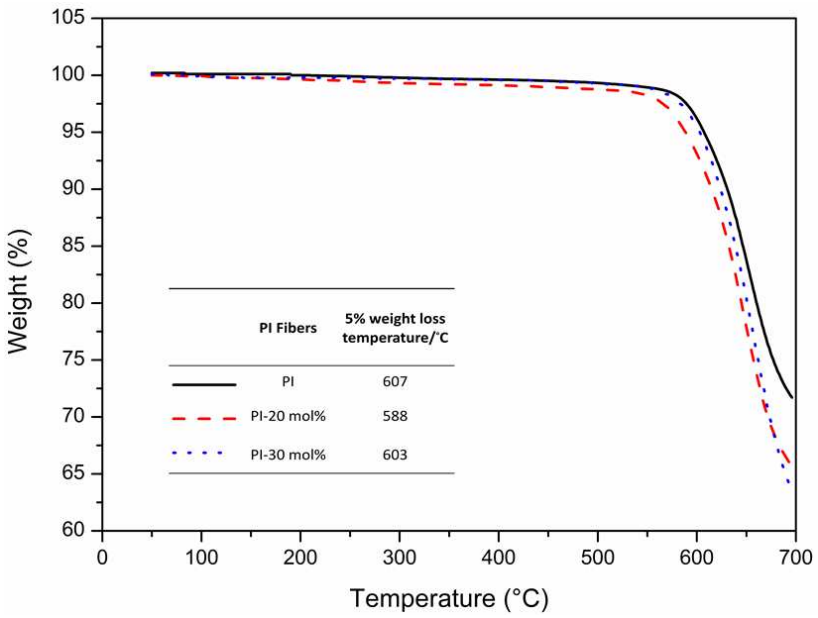

Fig. 7 TGA curves of the PI fibers with different amount of dehydration reagents in nitrogen atmosphere

3.2 Effect of different PAA concentrations on the structures and properties of polyimide fibers

3.2.1 FT-IR analysis

The chemical structures of PAA and the final PI fibers prepared with different concentrations of PAA solutions are illustrated in Fig. 8. After the addition of 20 mol% dehydration reagents, the PAA fibers were partially imidized as shown in Fig. 8(a), in which the characteristic absorption bands of PI fibers are observed at 1773, 1715, 1369 and 740 cm^{-1}, attributing to the C=O asymmetrical stretching, C=O symmetrical stretching, C-N stretching and C=O bending of imide ring, respectively. For PI fibers displayed in Fig. 8(b), the fibers exhibit same absorption bands, indicating that the PI fibers derived from different concentrations of PAA solutions possess the same chemical structures. Additionally, it should be noted that high PAA concentration will accelerate the *pre*-imidization process, and therefore, the IDs of the PAA and PI fibers should be evaluated. Based on eqn (1), the IDs were calculated as summarized in Table 3. The PAA fibers prepared with high PAA concentration exhibit relatively high ID, indicating that high concentration facilitates the *pre*-imidization process, which is in well accordance with our expectations. Meanwhile, the ID of PI fibers also increases with the increased PAA concentrations, which is beneficial to improve the mechanical performances of the resulting PI fibers.

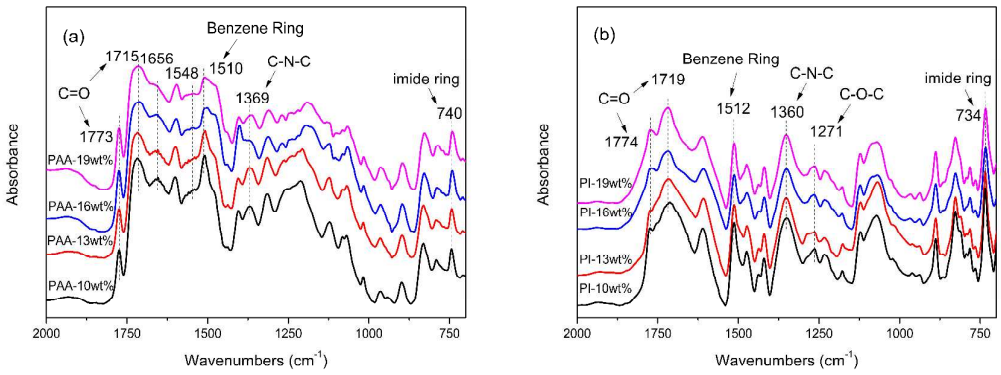

Fig. 8 FT-IR curves of the (a) PAA-PI and (b) PI fibers with different PAA concentrations

3.2.2 Mechanical properties

The IDs, intrinsic viscosities of the PAA solutions, linear density and mechanical properties of the corresponding PI fibers prepared with different PAA concentrations after *pre*-imidization process are collected in Table 3. It can be concluded that the PAA concentration has a tremendous effect on the intrinsic viscosities of PAA solutions and mechanical properties of PI fibers. The tensile strength and initial modulus of PI fibers increase from 0.72 to 1.21 GPa and 42.2 to 99.9 GPa when the PAA concentration increases from 10 to 19 wt%, respectively. Usually, low PAA concentration yields the decreased reactivity and suppresses the intermolecular cyclization in the *pre*-imidization process, thus resulting in the low IDs and intrinsic viscosities simultaneously. Similarly, the increased intrinsic viscosities of the PAA solutions induced by the increase of PAA concentration lead to the increased linear density of the PI fibers. Above all, the effectively enhanced mechanical properties of PI fibers is suggested to be mainly derived from the gradually ordered molecular arrangement and homogeneous structures induced by different PAA concentrations.

Table 3 The IDs, intrinsic viscosities of the PAA solutions, linear density and mechanical properties of the corresponding PI fibers with different PAA concentrations

PAA Concentration (wt%)	ID of PAA fibers (%)	ID of PI fibers (%)	Intrinsic Viscosity (dL g^{-1})	Linear Density (dtex)	Mechanical properties of the PI fibers		
					Tensile Strength (GPa)	Initial Modulus (GPa)	Elongation (%)
10	12.8	92.5	1.10	241.0	0.72±0.05	42.2±2.6	1.89±0.12
13	14.3	96.2	1.21	259.5	1.04±0.03	63.7±1.9	1.72±0.05
16	16.8	97.4	1.51	271.0	1.15±0.01	89.6±1.9	1.40±0.07
19	18.2	100	1.57	289.5	1.21±0.04	99.9±1.7	1.25±0.01

3.2.3 Molecular packing

The WAXD measurements were also performed for the PAA fibers prepared with different PAA concentrations as shown in Fig. 9. All the fibers exhibit a broad peak in the range of 5-40 °, and the intensity of the peak increases along with the increasing ID of the fibers. Herein, the order degree *X* of the macromolecules was quantitatively calculated to be 1.73 U_0/I_0, 2.96 U_0/I_0, 3.68 U_0/I_0 and 4.45 U_0/I_0 for PAA-10 wt%, PAA-13 wt%, PAA-16 wt% and PAA-19 wt% fibers according to eqn (2), respectively. The increased value represents the improved molecular alignment in the fibers during *pre*-imidization process. In the case of different PAA concentrations, the PAA solutions with low concentration will give rise to the intense dual-diffusion effect, thus posting a negative impact on the regular molecular packing in the fibers. Similarly, the curve-fitting WAXD profiles of the PI fibers are illustrated in Fig. 10. The PI fibers exhibit strong diffraction peaks after *pre*-imidization process, suggesting the formation of gradually ordered and oriented molecular packing patterns. After seperating the crystallization and amorphous contributions by deconvolution of the curves, the crystallinity of all the samples was found to be 32.0, 34.6, 35.1 and 38.4 % with the increased ID according to eqn (3). The crystallinity of the PI fibers were mainly determined by the induction of the gradually order-packed partially imidized PAA-PI fibers and enhanced by the thermal treatment process. In summary, the PI fibers prepared with high PAA concentration after *pre*-imidization treatment have better molecular arrangement, resulting in the outstanding mechanical properties of the resultant PI fibers.

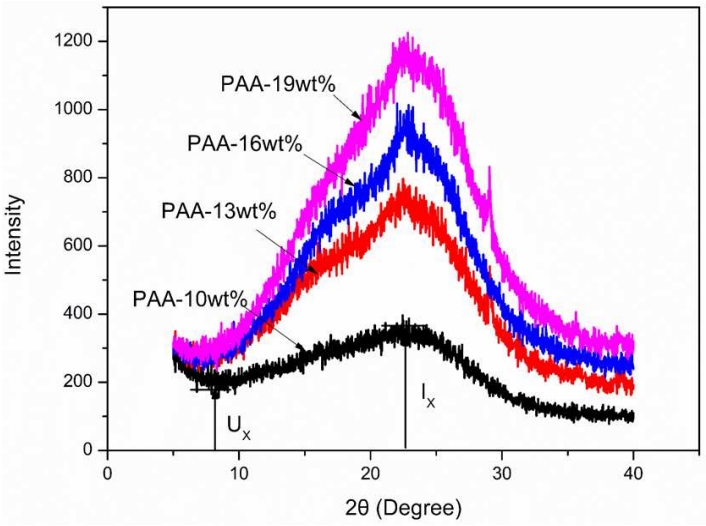

Fig. 9 The WAXD profiles of the PAA fibers with different PAA concentrations

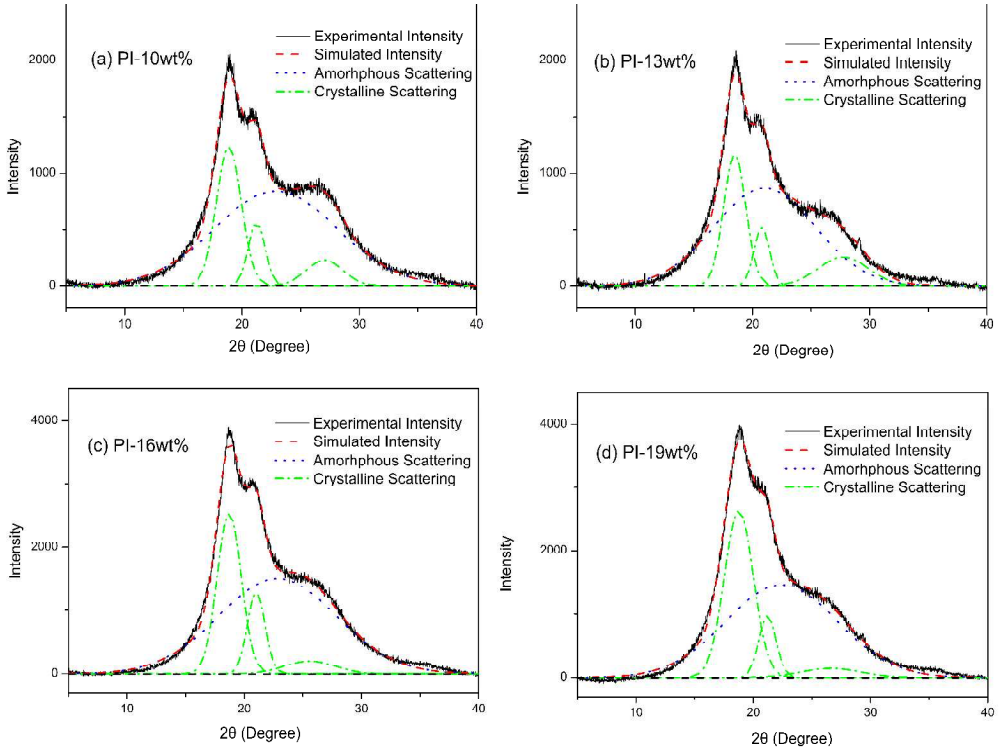

Fig. 10 The WAXD peak fitting profiles of the PI fibers with different PAA concentrations

3.2.4 Morphology

Fig. 11 shows the surface morphologies (a_1-d_1) of the PI fibers and fractured cross-section morphologies (a_2-d_2) of PAA fibers with different PAA concentrations. Similarly, all the PI fibers exhibit homogeneous and smooth surface with different PAA concentrations, which confirms the outstanding mechanical properties of the resulting PI fibers. As for fractured cross-section morphologies, all the PAA fibers exhibit regular circle morphologies except for PAA-10 wt% fibers, which is critically dependent on the dual-diffusion process. As mentioned above, low PAA concentration gives rise to intense dual-diffusion effect and therefore, leading to the irregular cross-section shape of the PAA fibers and the presence of adhesion between the fibers. In summary, it can be concluded that the increase of PAA concentration contributes to the homogeneous surface and uniform cross-section morphologies of the fibers in the present work, which is of great importance in preparing high-performance PI fibers.

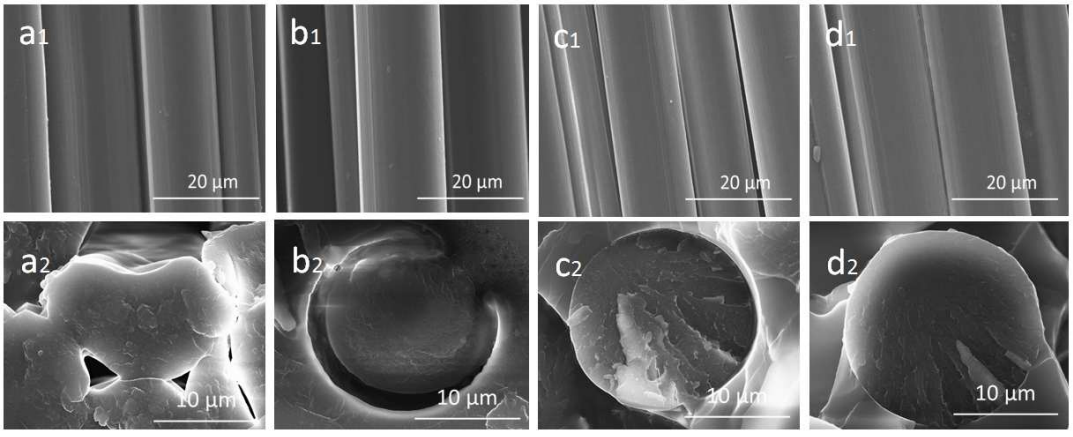

Fig. 11 The surface morphologies (a_1-d_1) of the PI fibers and fractured cross-section morphologies (a_2-d_2) of PAA fibers with different PAA concentrations.

(a) 10 wt%; (b) 13 wt%; (c) 16 wt%; (d) 19 wt%

The 2D SAXS patterns of PI fibers with different PAA concentrations are obtained in Fig. 12. The intense scattering along the meridian directions is mainly attributed to the existence of microvoids in the fibers, since there is no detectable microfibrillar scattering in the SAXS patterns.[33] Moreover, substantial changes have occured on the parameters of microvoids such as average radius R, length L and misorientation B_{Φ} with different PAA concentrations, which are of great significance to the mechanical properties of PI fibers.

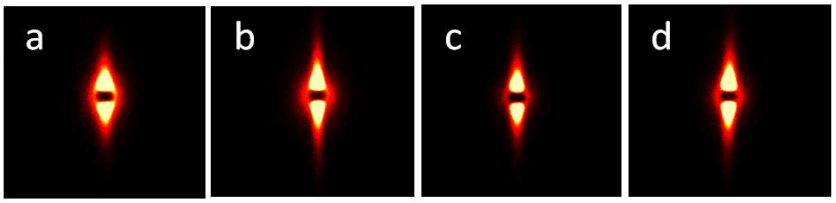

Fig. 12 2D SAXS patterns of the PI fibers with different PAA concentrations.

(a) PI-10 wt%; (b) PI-13 wt%; (c) PI-16 wt%; (d) PI-19 wt%

The strong scattering of the PI fibers with different PAA concentrations, as depicted in Fig. 13(a), giving evidence of the presence of microvoids with nanoscale structures. In the same manner, the radius of the microvoids can be calculated followed by the Guinier functions, and the Guinier plot of PI-10 wt% fibers is presented in Fig. 13(b) as the representative. Also, the length and misorientation of the microvoids are determined according to Ruland, and the corresponding plots of PI-10 wt% fibers are shown in Fig. 13(c) and 13(d). From the results listed in Table 4, the size of the microvoids is evidently decreased with the increased PAA concentrations, and the smallest volume of microvoids is obtained for PI-19 wt% fibers. The varied size of the

microvoids is ascribed to the difference in dual-diffusion process. During the process, the solvent diffuses into the coagulation bath and the coagulant diffuses into the fibers. Nevertheless, the fibers prepared with low PAA concentration contain too much solvent, which facilitates the mass transfer process and therefore, resulting in large size of microvoids in the fibers. Above all, with the increased PAA concentration, the homogeneous structures are gradually formed, which should be responsible for the improved mechanical properties of PI fibers.

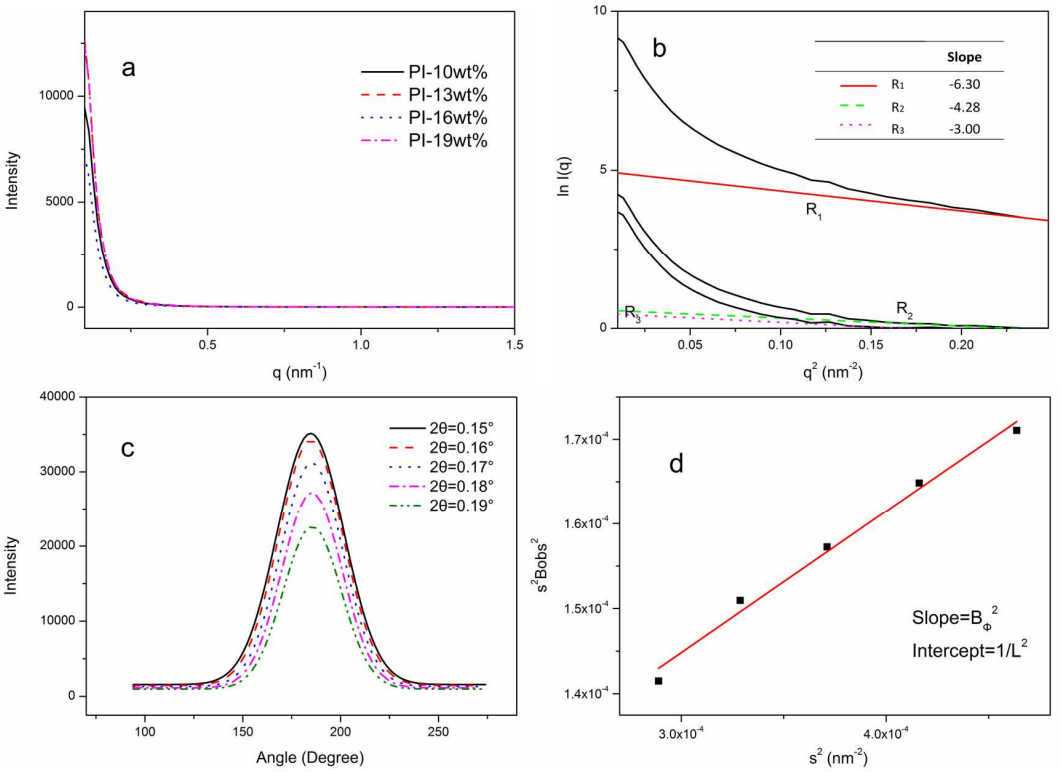

Fig. 13 (a) SAXS profiles of the PI fibers with different PAA concentrations; (b) Guinier plot of the scattered intensities of PI-10 wt% fibers along the meridian direction by Fankuchen successive tangent method; (c) Intensity profiles corresponding to azimuthal scans at different scattering vectors of the PI-10 wt% fibers; (d) Ruland plot of the PI-10 wt% fibers

Table 4 The parameters of microvoids of the PI fibers with different PAA concentrations

PI Fibers	R_i						R (nm)	L (nm)	B_Φ (°)
	R_1 (nm)	W_1	R_2 (nm)	W_2	R_3 (nm)	W_3			
PI-10 wt%	2.15	1.00	1.48	0.29	1.77	0.12	2.81	110.77	23.39
PI-13 wt%	2.09	1.00	1.59	0.22	0.92	0.30	2.71	105.47	19.41
PI-16 wt%	2.12	1.00	1.66	0.24	1.53	0.10	2.67	102.71	19.19
PI-19 wt%	2.04	1.00	1.40	0.27	1.25	0.19	2.66	102.54	18.04

3.2.5 Thermal properties

The thermal-oxidative stabilities of the PI fibers prepared with different PAA concentrations were also examined by TGA measurements as illustrated in Fig. 14. A typical one-step thermal degradation behavior under a nitrogen atmosphere is presented for all the PI fibers. The fibers exhibit excellent thermal-oxidative stabilities with the 5 % weight loss temperature above 610 °C, meanwhile, the value increases along with the increased PAA concentrations. It is essential to mention that the thermal-oxidative stabilities of the PI fibers are enhanced as a result of the increased imidization degree of the PI fibers, since the imidization degree of the PI fibers is also of importance in controlling the mechanical properties of the resultant PI fibers.

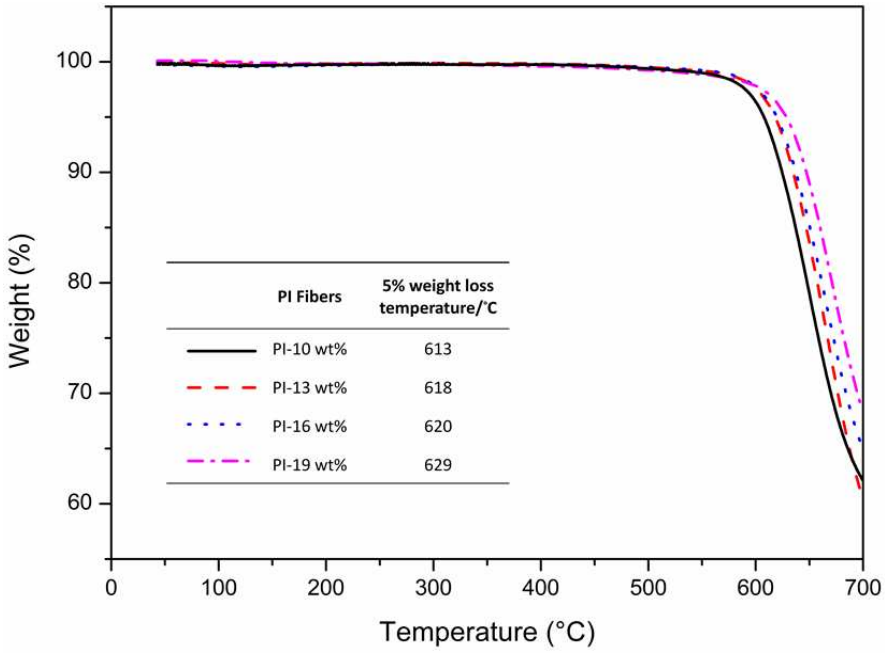

Fig. 14 TGA curves of the PI fibers with different PAA concentrations in nitrogen atmosphere

4 Conclusion

A series of PI fibers were prepared from the combination of BPDA, ODPA and *p*-PDA via the *pre*-imidization process and a typical two-step wet-spinning method. Both the different amount of dehydration reagents and PAA concentrations were adopted to examine the structures and properties of the final PI fibers. The results showed that both the increased amount of dehydration reagents and PAA concentrations led to the effectively enhancement in the mechanical properties of PI fibers. The PI fibers prepared with 30 mol% dehydration reagents exhibited the tensile strength of 1.61 GPa and initial modulus of 106.2 GPa, while the fibers obtained with 19 wt% PAA concentration possessed the tensile strength of 1.21 GPa and initial modulus of 99.9 GPa. Similarly, the *pre*-imidization process resulted in the ordered molecular arrangement of the polymer chains and gradually formed homogeneous structures in the

fibers, which were deduced to be the main reasons for the improved mechanical properties of PI fibers. On the other hand, the fibers prepared with the *pre*-imidization process possessed excellent thermal stabilities, although the 5 % weight loss temperature was slightly reduced as compared with that of the pure PI fibers as a result of the residual dehydration reagents in the fibers. In conclusion, the present work provided a new approach in obtaining high-performance PI fibers through the *pre*-imidization process.

Acknowledgements

The authors greatly thank the financial support from the National Natural Science Foundation of China (NSFC, Project No.51373008), National Key Basic Research Program of China (973 Program, No.2014CB643606), Higher School Specialized Research Fund for Doctoral Priority Areas of Development Project (No.20130010130001) and Fundamental Research Funds for the Central Universities of China (Project No.ZY1408).

Notes and References

1. W. E. Dorogy and A. K. St Clair, *Journal of applied polymer science*, 1991, **43**, 501-519.
2. W. E. Dorogy and A. K. S. Clair, *Journal of applied polymer science*, 1993, **49**, 501-510.
3. M. Hasegawa and K. Horie, *Progress in Polymer Science*, 2001, **26**, 259-335.

4. R. Dine‐Hart and W. Wright, *Journal of Applied Polymer Science*, 1967, **11**, 609-627.

5. M. Ding, *21st Century SP's Series in Chemistry*, 2006, 571-588.

6. M. Bessonov, *Polyimides--thermally stable polymers*, Consultants Bureau, 1987.

7. D. Wilson, H. Stenzenberger and P. Hergenrother, *Glasgow and London*, 1990.

8. M. Ghosh, *Polyimides: fundamentals and applications*, CRC Press, 1996.

9. H. Niu, S. Qi, E. Han, G. Tian, X. Wang and D. Wu, *Materials Letters*, 2012, **89**, 63-65.

10. H. Niu, M. Huang, S. Qi, E. Han, G. Tian, X. Wang and D. Wu, *Polymer*, 2013, **54**, 1700-1708.

11. S. Z. Cheng, Z. Wu and E. Mark, *Polymer*, 1991, **32**, 1803-1810.

12. M. Eashoo, D. Shen, Z. Wu, C. J. Lee, F. W. Harris and S. Z. Cheng, *Polymer*, 1993, **34**, 3209-3215.

13. J. Dong, C. Yin, Z. Zhang, X. Wang, H. Li and Q. Zhang, *Macromolecular Materials and Engineering*, 2014, **299**, 1170-1179.

14. S. Huang, Z. Jiang, X. Ma, X. Qiu, Y. Men, L. Gao and M. Ding, *Plastics, Rubber and Composites*, 2013, **42**, 407-415.

15. C. Yin, J. Dong, Z. Zhang, Q. Zhang and J. Lin, *Journal of Polymer Science Part B: Polymer Physics*, 2015, **53**, 183-191.

16. J. Dong, C. Yin, J. Lin, D. Zhang and Q. Zhang, *RSC Advances*, 2014, **4**, 44666-44673.

17. L. Luo, J. Yao, X. Wang, K. Li, J. Huang, B. Li, H. Wang and X. Liu, *Polymer*, 2014, **55**, 4258-4269.

18. T. Kaneda, T. Katsura, K. Nakagawa, H. Makino and M. Horio, *Journal of applied polymer science*, 1986, **32**, 3133-3149.

19. T. Kaneda, T. Katsura, K. Nakagawa, H. Makino and M. Horio, *Journal of applied polymer science*, 1986, **32**, 3151-3176.

20. J. Chang, H. Niu, M. Zhang, Q. Ge, Y. Li and D. Wu, *Journal of Materials Science*, 2015, **50**, 4104-4114.

21. Y. Wang, Y. Yang, Z. Jia, J. Qin and Y. Gu, *Polymer*, 2012, **53**, 4157-4163.

22. V. Smirnova, I. Gofman, V. Lavrent'Ev and V. Sklizkova, *Polymer Science Series A*, 2007, **49**, 1114-1119.

23. Y. Zhai, Q. Yang, R. Zhu and Y. Gu, *Journal of Materials Science*, 2008, **43**, 338-344.

24. M. Marek, P. Schmidt, B. Schneider, B. Bednář and J. Králíček, *Die Makromolekulare Chemie*, 1990, **191**, 2631-2637.

25. Y. Zhuang, X. Liu and Y. Gu, *Polymer Chemistry*, 2012, **3**, 1517-1525.

26. X. Liu, G. Gao, L. Dong, G. Ye and Y. Gu, *Polymers for Advanced Technologies*, 2009, **20**, 362-366.

27. R. Sengupta, V. Tikku, A. K. Somani, T. K. Chaki and A. K. Bhowmick, *Radiation physics and Chemistry*, 2005, **72**, 625-633.

28. R. Snyder, B. Thomson, B. Bartges, D. Czerniawski and P. Painter, *Macromolecules*, 1989, **22**, 4166-4172.

29. X. Chen, C. Burger, F. Wan, J. Zhang, L. Rong, B. S. Hsiao, B. Chu, J. Cai and L. Zhang, *Biomacromolecules*, 2007, **8**, 1918-1926.

30. G. Jiang, W. Huang, L. Li, X. Wang, F. Pang, Y. Zhang and H. Wang, *Carbohydrate Polymers*, 2012, **87**.

31. G. Jiang, Y. Yuan, B. Wang, X. Yin, K. S. Mukuze, W. Huang, Y. Zhang and H. Wang, *Cellulose*, 2012, **19**, 1075-1083.

32. M. H. Jellinek, E. Soloman and I. Fankuchen, *Industrial & Engineering Chemistry Analytical Edition*, 1946, **18**, 172-175.

33. S. Ran, D. Fang, X. Zong, B. Hsiao, B. Chu and P. Cunniff, *Polymer*, 2001, **42**, 1601-1612.

34. W. Ruland, *Journal of Applied Physics*, 1967, **38**, 3585-3589.

35. R. Perret and W. Ruland, *Journal of Applied Crystallography*, 1970, **3**, 525-532.

Figure Captions

Scheme 1 The synthetic route of PI fibers

Figure 1 FT-IR curves of the (a) PAA and (b) PI fibers with different amount of dehydration reagents

Figure 2 The WAXD profiles of the PAA fibers with different amount of dehydration reagents

Figure 3 The WAXD peak fitting profiles of the PI fibers with different amount of dehydration reagents

Figure 4 The surface morphologies (a-c) of the PI fibers and fractured cross-section morphologies (d-f) of PAA fibers with different amount of dehydration reagents. (a) PI; (b) PI-20 mol%; (c) PI-30 mol%; (d) PAA; (e) PAA-20 mol%; (f) PAA-30 mol%

Figure 5 2D SAXS patterns of the PI fibers with different amount of dehydration reagents. (a) PI; (b) PI-20 mol%; (c) PI-30 mol%

Figure 6 (a) SAXS profiles of the PI fibers with different amount of dehydration reagents; (b) Guinier plot of the scattered intensities of PI-20 mol% fibers along the meridian direction by Fankuchen successive tangent method; (c) Intensity profiles corresponding to azimuthal scans at different scattering vectors of the PI-20 mol% fibers; (d) Ruland plot of the PI-20 mol% fibers.

Figure 7 TGA curves of the PI fibers with different amount of dehydration reagents in nitrogen atmosphere

Figure 8 FT-IR curves of the (a) PAA and (b) PI fibers with different PAA concentrations

Figure 9 The WAXD profiles of the PAA fibers with different PAA concentrations

Figure 10 The WAXD peak fitting profiles of the PI fibers with different PAA concentrations

Figure 11 The surface morphologies (a_1-d_1) of the PI fibers and fractured cross-section morphologies (a_2-d_2) of PAA fibers with different PAA concentrations. (a) 10 wt%; (b) 13 wt%; (c) 16 wt%; (d) 19 wt%

Figure 12 2D SAXS patterns of the PI fibers with different PAA concentrations. (a) PI-10 wt%; (b) PI-13 wt%; (c) PI-16 wt%; (d) PI-19 wt%

Figure 13 (a) SAXS profiles of the PI fibers with different PAA concentrations; (b) Guinier plot of the scattered intensities of PI-10 wt% fibers along the meridian direction by Fankuchen successive tangent method; (c) Intensity profiles corresponding to azimuthal scans at different scattering vectors of the PI-10 wt% fibers; (d) Ruland plot of the PI-10 wt% fibers.

Figure 14 TGA curves of the PI fibers with different PAA concentrations in nitrogen atmosphere

Table Captions

Table 1 The IDs, intrinsic viscosities of the PAA solutions, linear density and mechanical properties of the corresponding PI fibers with different amount of dehydration reagents

Table 2 The parameters of microvoids of the PI fibers with different amount of dehydration reagents

Table 3 The IDs, intrinsic viscosities of the PAA solutions, linear density and mechanical properties of the corresponding PI fibers with different PAA concentrations

Table 4 The parameters of microvoids of the PI fibers with different PAA concentrations